Cochleate formulations of Amphotericin b designed for oral administration using a naturally occurring phospholipid

Antonio Lipa-Castro, Valérie Nicolas, Angelina Angelova, Ghozlene Mekhloufi, Bastien Prost, Monique Chéron, Vincent Faivre, Gillian Barratt

International Journal of Pharmaceutics xxx (xxxx) 120688

Contents lists available at ScienceDirect

International Journal of Pharmaceutics

journal homepage: www.elsevier.com/locate/ijpharm

Cochleate formulations of amphotericin b designed for oral administration using a naturally occurring phospholipid

Antonio Lipa-Castro [a], Valérie Nicolas [b], Angelina Angelova [a], Ghozlene Mekhloufi [a], Bastien Prost [c], Monique Chéron [d], Vincent Faivre [a], Gillian Barratt [a,*]

[a] Université Paris-Saclay, CNRS, Institut Galien Paris-Saclay, 92290 Châtenay-Malabry, France
[b] Université Paris-Saclay, Inserm, IPSIT, Plateforme MIPSIT, 92290 Châtenay-Malabry, France
[c] Université Paris-Saclay, Inserm, IPSIT, Plateforme SAMM, 92290 Châtenay-Malabry, France
[d] Faculté de Pharmacie, Université Paris-Saclay, 92290 Châtenay-Malabry, France

ARTICLE INFO

Keywords:
Phosphatidylserine
Cochleates
Amphotericin B
Oral bioavailability
Caco2 cells
synchrotron SAXS
Circular dichroism

ABSTRACT

The purpose of this work is to formulate the poor soluble antifungal and antiparasitic agent Amphotericin B (AmB) in cost-effective lipid-based formulations suitable for oral use in developing countries, overcoming the limitations of poor water solubility, nephrotoxicity and low oral bioavailability. The antifungal agent was formulated, at different molar proportions, in cochleate nanocarriers prepared using an accessible naturally occurring phospholipid rich in phosphatidylserine (Lipoid PSP70). These nanoassemblies were prepared by condensation of negatively charged phospholipid membrane vesicles with divalent cations (Ca^{2+}). Small-angle X-ray scattering studies revealed the Ca^{2+}-triggered condensation of loosely packed multilamellar vesicles into tightly packed bilayers of strongly dehydrated multilamellar organization characterized by narrow Bragg peaks. Transmission electron microscopy and quasi-elastic light scattering studies demonstrated the formation of nanosized particles. AmB drug loading was above 55% in all formulations. Circular dichroism demonstrated the prevalence of monomeric and complexed forms of AmB over toxic aggregates. The stability of AmB in gastric medium was improved by loading in cochleates and its release in gastrointestinal media was retarded. Confocal microscopy studies revealed the *in-vitro* interactions of Lipoid PSP70-based cochleates with Caco2 intestinal cell monolayers. The results suggest that the low-cost AmB-loaded cochleates may increase the therapeutic range of this drug.

1. Introduction

Amphotericin B is a polyene antibiotic belonging to the macrolide family that is used to treat serious, life-threatening fungal infections as well as infections caused by the protozoan parasite *Leishmania* (Berman, 2005; Chattopadhyay & Jafurulla, 2011; No, 2016). AmB is poorly soluble in both water (10^{-7}M) and many organic solvents. It has a molecular mass of 924 g/mol and an estimated octanol/water partition coefficient of −2.80. In its pharmaceutical form sodium deoxycholate is used to solubilize the antibiotic in the form of mixed micelles (Fungizone®). However, instability of this form in the plasma gives rise to dose-limiting toxicity (notably nephrotoxicity and infusion-related reactions) (Espada et al., 2008; Huang et al., 2002). Lipid-based formulations, and in particular a liposomal speciality (AmBisome®; LAmB), can reduce toxicity but are expensive (Hamill, 2013). Furthermore, none of the commercial formulations provide significant bioavailability of AmB when administered by the oral route, due to the high molecular weight and poor water solubility of the drug. However, an orally

Abbreviations: AC, acyl chain; AmB, amphotericin B; BSA, bovine serum albumin; CD, circular dichroism; D_h, hydrodynamic diameter; DLS, dynamic light scattering; DMEM, Dulbecco's modified Eagle's medium; DMSO, dimethyl sulfoxide; DOPS, dioleoylphosphatidylserine; EDTA, ethylenediaminetetraacetic; FaSSIF, fasted state simulated intestinal fluid; FBS, foetal bovine serum; FeSSIF, fed state simulated intestinal fluid; HBSS, Hank's balanced salt solution; HPLC-MS, high-performance liquid chromatography coupled to electrospray mass spectrometry; MLV, multilamellar vesicles; MTT, methylthiazoltetrazolium; PBS, phosphate buffered saline; PdI, polydispersity index; PS, phosphatidylserine; Rho-PE, 1,2-dioleoyl-*sn*-glycero-3-phosphoethanolamine-N- (lissamine rhodamine B sulfonyl) (ammonium salt); SAXS, small-angle X-ray scattering; SGF, simulated gastric fluid; TEER, transepithelial electrical resistance; WAXS, wide-angle X-ray scattering

* Corresponding author.
E-mail address: gillian.barratt@u-psud.fr (G. Barratt).

https://doi.org/10.1016/j.ijpharm.2021.120688
Received 11 February 2021; Received in revised form 23 April 2021; Accepted 4 May 2021
0378-5173/

active formulation would be advantageous, particularly for the treatment of leishmaniasis in developing countries where this disease is endemic and presents a major public health problem (Torres-Guerrero et al., 2017).

Several experimental formulations have been reported to improve the bioavailability of AmB by the oral route (Faustino and Pinheiro, 2020). These have been based on mixed micelles (Chen et al., 2015), emulsions or self-emulsifying systems (Ibrahim et al., 2013; Khan et al., 2019), cubosomes (Jain et al., 2018; Yang et al., 2014), solid-lipid nanoparticles (Chaudhari et al., 2016) and chitosan-covered nanoparticles (Serrano et al., 2015). These formulations can prolong the residence time of the drug in the intestine and allow its release in the molecular form. Recently, a prodrug of AmB covalently linked to oleic acid was shown to increase the bioavailability of the drug by a factor of almost 5 after oral administration to rats (Thanki et al., 2019). This type of prodrug is designed to use physiological routes of lipid absorption.

One of the forms that has been most frequently exploited for the oral administration of AmB is cochleates (Lu et al., 2019; Santangelo et al., 2000; Zarif et al., 2000). These are stable phospholipid-cation precipitates that consist of cigar-like spiral rolls formed of negatively charged phospholipid bilayers with divalent metal counter ions as bridging agents between the bilayers. Due to the tightly rolled structure, they possess little or no aqueous phase, in contrast to liposomes. This dehydrated internal structure renders them an ideal vehicle for delivering lipid-soluble drugs, proteins or nucleic acids into biological systems because they protect the encapsulated material against enzymatic or chemical degradation (Pawar et al., 2015). As a highly hydrophobic molecule, AmB would be localized in the lipid bilayers of the tightly rolled cochleates and in this way would be protected from degradation when exposed to harsh environmental conditions and enzymes. Furthermore, it could be released in a form with a higher possibility of passing the intestinal barrier. Initial biodistribution studies of AmB encapsulated in cochleates administered orally in a mouse model showed that the cochleates could deliver therapeutic levels of AmB to target organs. Cures were observed after oral administration of AmB-loaded cochleates to mice infected with *Candida albicans* (Santangelo et al., 2000) or *Cryptococcus neoformans* (Lu et al., 2019). A phase II clinical trial was recently undertaken in patients with mucocutaneous candidiasis (Aigner and Lass-Flörl, 2020). Low toxicity was observed, but the improvement in symptoms was not better than that observed with fluconazole.

Despite the encouraging results with AmB-loaded cochleates that have been obtained over the last decades, their use for the treatment of leishmaniasis has not been developed. The negatively charged phospholipid most commonly employed for the formation of cochleates is phosphatidylserine (PS). Often, the synthetic 18-carbon monounsaturated 1,2-dioleoyl-*sn*-glycero-3-phospho-L-serine (DOPS) is chosen. However, this synthetic lipid is expensive, limiting the use of such formulations in the developing countries where leishmaniasis is prevalent. The objective of this study was to develop cochleate formulations using a naturally occurring phosphatidylserine from soy (Lipoid PSP70) able to encapsulate AmB and to evaluate their suitability for oral administration. Different molar proportions of AmB within the cochleates were evaluated for its influence on the shape, size and internal structure of the cochleates. The aggregation state of the AmB, its stability in the gastric environment, its *in-vitro* release and its toxicity to intestinal cells were also investigated.. Lastly, studies of interactions with Caco2 cells were carried out by confocal microscopy.

2. Materials and methods

2.1. Materials

DOPS, Lipoid PSP70 and lecithin were gifts from Lipoid (Grasse, France). AmB and sodium taurocholate were purchased from Alfa Aesar™. Cholesterol, vitamin E, dextran (500,000 Da), poly (ethylene glycol) (PEG 8000), ethylenediaminetetraacetic (EDTA), calcium chloride, glucose, sodium chloride, potassium chloride, magnesium sulphate, Tris base, pepsin, Tween 80, sodium hydroxide, sodium chloride, sodium dibasic phosphate, sodium bicarbonate, potassium monobasic phosphate and sodium monobasic phosphate were purchased from Sigma-Aldrich. AMBERLITE™ 200CNa resin was a gift from Dow Water & Process. Methanol, chloroform, isopropanol, heptane, acetic acid, hydrochloric acid and other solvents were purchased from Merck. Water was purified by reverse osmosis (Milli-Q Millipore). Dulbecco's modified Eagle's medium (DMEM), phosphate buffered saline (PBS), foetal bovine serum (FBS), non-essential amino acids solution (10 mM, 100x), penicillin–streptomycin solution (10,000 units/mL penicillin and 10 mg/mL of streptomycin), trypsin-EDTA solution (0.05% trypsin, 0.53 mM EDTA), methylthiazoltetrazolium (MTT), FITC-dextran 4.4 kDa, FITC-labelled phalloidin and dimethyl sulfoxide were obtained from Sigma-Aldrich. The fluorescent phospholipid 1,2-dioleoyl-*sn*-glycero-3-phosphoethanolamine-N- (lissamine rhodamine B sulfonyl) (ammonium salt) was obtained from Avanti Polar Lipids (Alabaster, Alabama, USA). Corning Transwell® inserts of 12 mm diameter, with 0.4 μm pore-size polyester membranes, and 24 mm diameter, with 0.4 μm pore-size polycarbonate membranes, were purchased from the Costar Corning Corporation (New York, USA).

2.2. Ion exchange treatment of the Lipoid PSP70

Lipoid PSP70 was obtained as a calcium salt that was insoluble in organic solvent. Therefore, an ion exchange treatment was necessary to convert it to the sodium salt. 1 g of Lipoid PSP70 was dissolved in chloroform/methanol/water (20/10/2) at a concentration of 5 mg/mL, after which 75 g of resin (previously dried over 24 h at 50 °C due to its high water content) was added and stirred for 12 h. The suspension was filtered (PTFE 0.2 μm) and the solvent was removed by vacuum evaporation (Buchi R-210 Rotavapor System). The lipid film was recovered in chloroform/methanol/water (20/10/2) solvent to obtain a concentration of 5 mg/mL of lipid. A second exchange treatment was performed with 10 g of resin stirred for 2 h. The suspension was filtered and the solvent removed by vacuum evaporation. Finally, the lipid film was recovered in chloroform/methanol (60/40) at 5 mg/mL total lipid concentration.

Identification and quantification of phosphatidylserine were carried out by normal phase high-performance liquid chromatography coupled to electrospray mass spectrometry (HPLC-MS). The analysis was done by coupling a quaternary RSLC Dionex-U3000 liquid chromatography (Thermo Scientific) with a Corona-CAD Ultra aerosol charge detector (Thermo Scientific) and a hybrid mass spectrometer equipped with ion trap and an orbital trap LTQ- Orbitrap Velos Pro (Thermo Scientific) for PS species identification. The separation was performed on an YMC PVA-Sil column (150 mm × 2.1 mm I.D., 5 μm particles, pore size 120 Å). The column was operated under gradient conditions with mobile phase A: heptane/ Isopropanol 98/2, mobile phase B: chloroform/ Isopropanol 65/35, mobile phase C: methanol/ water 95/5 and mobile phase D: Isopropanol where A, B and C contained 1% acetic acid and 0.08% triethylamine. The quaternary gradient program used is shown in Table S1. The flow rate was 400 μL/min and the injection volume was 5 μL. Absolute ethanol was added with a second mixing tee, with a flow rate of 200 μL/min to increase the flow entering the Corona CAD and thereby maintain aerosol stability. All data corresponding to mass spectrometry were collected in negative ionization mode. Fullscan high resolution MS (HRMS) was performed in the orbitrap with a scan range of m/z 300–1800 and a resolution of 100,000 and data-dependent MS^2 and MS^3 with collision-induced dissociation in the CID (Collision Induced Dissociation) fragmentation. Acyl chain (AC) composition of the different PS species was performed

in negative ESI data-dependent mode in the LTQ ion trap (low resolution) (Moulin et al., 2015).

2.3. Preparation of AmB-loaded cochleates

The molar proportions of Lipoid PSP70 and cholesterol of 9/2 were established based on the impact on the internal structure of cochleates determined by SAXS and on the stability of AmB in gastric medium (Supplementary Figure S1 and Table S2 respectively). Thereafter, cochleates were prepared by the hydrogel isolation method (Zarif et al., 2000) using Lipoid PSP70, cholesterol and vitamin E (as antioxidant) in molar proportions of 9/2/0.01 with AmB at four different molar ratios: 0.5, 1, 2 and 3. The molecular weight of Lipoid PSP70, containing a mixture of acyl chains, was considered to be the same as that of the sodium salt of dioleoylphosphatidylserine: 810 g/mol. The formulations will be designated as follows in the text and illustrations below:

F0.5: 9 Lipoid PSP70/2 cholesterol/0.06 vitamin E/0.5 AmB
F1: 9 Lipoid PSP70/2 cholesterol/0.06 vitamin E/1 AmB
F2: 9 Lipoid PSP70/2 cholesterol/0.06 vitamin E/2 AmB
F3: 9 Lipoid PSP70/2 cholesterol/0.06 vitamin E/3 AmB

Since AmB is photosensitive, all procedures were carried out in a way that protected it from light as much as possible. Amber glassware was used when possible and when not it was covered with aluminium foil. All equipment used was shielded from light.

Firstly, small unilamellar liposomes were formed by film hydration. Lipoid PSP70, cholesterol, vitamin E dissolved in chloroform/methanol (60/40) and AmB dissolved in alkaline methanol (containing sodium hydroxide solution at 1 mM) were mixed in the desired proportions, dried by rotary evaporation and hydrated with 0.05 M Tris buffer pH 7.4 to a lipid concentration of 5.6 mM. The size was reduced and homogenized by probe sonication (Bioblock Scientific vibracell 72,441 ultrasons) with a sonic power of 2 for 7 cycles of 1 min at 1-min intervals over ice followed by sequential extrusion on calibrated membranes (Whatman® Nuclepore) to form liposomes with a mean diameter of about 100 nm. Non-encapsulated AmB was retained on the membranes at this stage.

To form cochleates, the liposomes were mixed with 40% (w/w) dextran in a suspension of 2/1 (v/v) dextran/liposome and injected into 15% (w/w) polyethylene glycol 8000 with stirring. $CaCl_2$ solution was added at a final concentration of 50 mM, and stirring was continued for 15 min to form cochleates. The cochleates were recovered by filtration followed by washing with 1 mM $CaCl_2$/150 mM NaCl and freeze-drying for 24 h in the dark to avoid photodegradation (Freeze dryer CRYOTEC Cosmo 20 K-80). Unloaded cochleates (designated F0) were prepared in the same way without addition of AmB. Rhodamine-labeled unloaded cochleates were prepared by including 1,2-dioleoyl-*sn*-glycero-3-phosphoethanolamine-N- (lissamine rhodamine B sulfonyl) ammonium salt (Rho-PE)) at 0.2% molar ratio with Lipoid PSP70, thereby obtaining cochleates with the composition 9 Lipoid PSP70 /2 cholesterol /0.018 Rho-PE/ 0.06 vitamin E.

2.4. Electronic microscopy

A transmission electron microscope operating at 120KV (JEOL JEM-1400) at the I2BC (Gif-sur-Yvette, France) was used to examine the aggregation state and morphology of the nanoparticles obtained with Lipoid PSP70. The cochleates were suspended in 2 mM $CaCl_2$ solution at 0.4 mg/mL, after which 5 µL of the solution was deposited on a copper grid covered with a formvar film (400 mesh) for 1 h until air-dried followed by negative staining treatment with 1% sodium phosphotungstate. Excess solution was removed with filter paper from the back of the grids before observation. Images were acquired using a high-resolution camera (Orius SC1000).

2.5. Morphogranulometry

The aggregation state and morphology of the cochleates obtained from Lipoid PSP70 were also analyzed by flow imaging microscope, using a Flow-Cell 200 S-M instrument (Occhio, Belgium) morphogranulometer. The cochleate suspension was pumped through a 50-µm-wide flow cell and digital images were obtained with a high-resolution camera with a 0.185-µm spatial resolution (9 × zoom factor). Cochleate samples were suspended in 2 mM $CaCl_2$ solution at 0.8 mg/mL. Images were acquired when the flow was completely stopped to ensure good resolution. The morphogranulometer was equipped with image analysis software Callisto (Occhio, Belgium) designed for particle detection using the grey level difference between the particle and background.

2.6. Size, polydispersity index and zeta potential analysis

The hydrodynamic diameters (D_h), polydispersity indexes (PdI) and zeta potential of the formulations obtained from Lipoid PSP70 as liposomes and cochleates were studied by dynamic light scattering (DLS) measurements using a Zetasizer Nano ZS90 instrument (Malvern, France). The liposomes were diluted in Tris 0.05 M pH 7.4 and cochleates were dispersed in NaCl/$CaCl_2$ 150 mM/ 1 mM solution. Zeta potential measurements were carried out after dilution of the liposomes in Tris (0.0125 M pH 7.4) and cochleates in $CaCl_2$ solution (2 mM). All measurements were performed in triplicate at 25 °C at a detection angle of 90° for size measurements.

2.7. Determination of AmB content by HPLC and encapsulation efficiency

The AmB content of the formulations was measured by reversed phase HPLC, using the method reported by Ménez et al., (2006a). This was performed with a HPLC system equipped with a quaternary 600 Controller pump, UV–Visible spectrophotometric detector (2996 Photodiode Array Detector, Waters) and an automatic injector (717 Autosampler, Waters). The column was a Symmetry® C_{18} column 150 mm × 4.6 cm, 5 µm particle size and 100 Å pore size (Waters). The mobile phase was 0.5% aqueous solution of triethylamine (adjusted to pH 5.2 with formic acid), acetonitrile and tetrahydrofuran (1000/385/154 v/v). The flow rate was 1 mL/min and the injection volume was 100 µL. The column temperature was 30 °C and the injection system was at room temperature. AmB was quantified using the peak areas acquired at 408 nm, with a retention time of about 9 min. A calibration curve was prepared from a series of dilutions of an AmB reference standard in MeOH/H_2O (1/1) in the range between 0.1 and 5 µg/mL. The correlation coefficient (R^2) was 0.9995, the limit of detection was 40 ng/mL and the limit of quantification was 100 ng/mL. Cochleate samples were treated with EDTA 0.05 M and MeOH to extract the AmB then diluted in MeOH/H_2O (1/1). Finally, samples were centrifuged with a VWR Galaxy Mini Centrifuge C1413 8 (2000 × g, 10 min) to remove the impurities. This treatment was sufficient to destroy the cochleate structure and ensure that AmB was present in its molecular form.

Since AmB is very poorly soluble in water, any non-encapsulated drug precipitated when the multilamellar liposomes were formed. These precipitates were retained on the extrusion membranes when the liposome size was reduced. Thus, the AmB recovered in the final cochleates could be considered as encapsulated. The encapsulation efficiency (EE %) for each preparation was calculated using the following equation:

$$EE\% = (Wt/Wi) \times 100\%$$

where Wt is the total amount of the AmB measured in the freeze-dried cochleates and Wi is the total quantity of AmB initially added to the

preparation. The AmB content was also expressed with respect to the total weight of freeze-dried cochleates that were recovered.

To confirm that the final cochleate preparation did not contain free AmB, an extraction procedure using 0.2% Tween 80 in 50 mM $CaCl_2$ solution was performed on formulations diluted to 2 μg/ml AmB content. This revealed that 5, 8, 11, and 12% of associated AmB could be extracted from F0.5, F1, F2 and F3 respectively. Thus, we can conclude that the majority of the AmB in the final cochleates was tightly associated with the lipid bilayers.

2.8. Small- and wide-angle X-ray scattering

For synchrotron SAXS measurements, liquid crystalline vesicular membranes and cochleate samples were introduced into X-ray capillaries with a diameter 1.5 mm and were sealed with paraffin wax. The experiments were performed at the SWING beamline of synchrotron SOLEIL (Saint Aubin, France) with a set-up previously described (David and Pérez, 2009). The samples were oriented in front of the X-ray beam (25 × 375 μm^2) using a designed holder for multiple capillaries positioning (X, Y, Z). The sample-to-detector distance was 3 m. The employed exposure time of 500 ms did not cause radiation damage. The q-vector was defined as $q = (4\pi/\lambda) \sin\theta$, where 2θ is the scattering angle. The synchrotron radiation wavelength was $\lambda = 1.033$ Å. The SAXS patterns were recorded with a two-dimensional Eiger X 4 M detector (Dectris) at 12 keV. The q-range calibration was done using a standard sample of silver behenate (d = 58.38 Å). Temperature was 22 °C. Data processing of recorded 2D images was performed by the FOXTROT software (David and Pérez, 2009). The interlamellar repeat distances, d, of the observed multilamellar structures were calculated from the positions of the Bragg peaks resolved in the SAXS patterns using the relationship $d = 2\pi/q$.

Additional SAXS patterns and some preliminary WAXS patterns were acquired using a microfocus X-ray tube (IμS, Incoatec), selecting the Cu Kα radiation. It was used with an intensity of 1000 μA and a voltage of 50 kV. The incident beam was focused at the detector with multilayer Montel optics and 2D Kratky block collimator. Small-angle (SAXS) and wide-angle (WAXS) X-ray scattering analyses were performed simultaneously using two position-sensitive linear detectors (Vantec-1, Bruker) set perpendicular to the incident beam direction, up to 7° (2θ) and at 19° to 28° (2θ) from it, respectively. The direct beam was stopped with a W-filter. The scattered intensity was reported as a function of the scattering vector $q = 4\pi \sin\theta/\lambda$ where θ is half the scattering angle and λ is the wavelength of the radiation. The repeat distances were calculated as above. Silver behenate and tristearin (β form) were used as standards to calibrate SAXS and WAXS detectors, respectively.

In order to prevent sedimentation, all the samples were suspended in 4% (w/w) dextran. Cochleates prepared from Lipoid PSP70 or DOPS, cholesterol and AmB in different ratios were compared. Multilamellar vesicles (MLV) from Lipoid PSP70 were also studied. All samples were introduced into thin-walled glass capillaries (GLAS, Müller, Berlin, Germany) of 1.5 mm external diameter which were then placed in a specially designed temperature-controlled sample holder (Microcalix, Setaram) maintained at 20 °C during the measurements. Acquisition time was 3600 s. Igor 6.03 was used for data processing.

2.9. Circular dichroism and UV–visible spectroscopy

The toxicity of AmB is related to the aggregation state of the molecules, which can be monitored by its absorbance spectrum in the UV/Vis range of 300–450 nm (Rochelle do Vale Morais et al., 2018). Therefore, the formulations were evaluated by UV–visible spectroscopy and circular dichroism. A JASCO J-810CD Spectropolarimeter (Tokyo, JAPAN and Jasco Spectra Manager v2 software were used for the record these parameters. Cochleates obtained from Lipoid PSP70 containing 3×10^{-5} M AmB (previously treated with 0.05 M EDTA) were put in 1-cm path length quartz cuvettes (Pham et al., 2014). Suspensions of cochleates without AmB at the same lipid composition and concentration were used as blanks. Furthermore, concentrated AmB in DMSO was diluted to 3×10^{-5} M in water as a control for the aggregated state of AmB and in methanol to obtain the monomeric state and examined under the same conditions. Measurements were conducted in triplicate at room temperature and the results for CD spectra are expressed as $\Delta\varepsilon$ ($M^{-1}.cm^{-1}$) (differential molar absorption dichroic coefficient) and the UV/Vis spectra are presented as molar extinction coefficient (ε, $M^{-1}.cm^{-1}$).

2.10. Stability of AmB in cochleates in gastric medium

It is known that AmB is unstable in the presence of gastric medium (Thanki et al., 2019). Therefore, its stability in the different formulations was studied using simulated gastric fluid (SGF). Samples of AmB-loaded cochleate formulations and a control of AmB dissolved in DMSO were suspended in SGF (0.32% w/v pepsin and pH adjusted to 1.2) (Pham et al., 2014) at an AmB concentration of 10 μg/mL and incubated at 37 °C under shaking at a speed of 75 rpm for 2 h. The suspension was immediately neutralised with the same volume of buffer (0.11 M NaOH, 0.03 M NaH_2PO_4 and 0.05 M EDTA) to pH 7, then 1 vol of MeOH was added followed by centrifugation in a VWR Galaxy Mini Centrifuge C1413 8 (2000 × g, 10 min). Finally, the supernatant was recovered to measure the AmB concentration by HPLC as described above. The amount of intact AmB recovered is expressed as a percentage of the original amount.

2.11. In-vitro release study

The *in-vitro* release of AmB-loaded cochleates was investigated under simulated gastro-intestinal conditions. The media were prepared as described by Pham et al (2014) with some modifications (Table S3). To ensure the solubility of released AmB in sink conditions, the initial concentration was low – 10 μg/mL, and Tween 80 was added to the gastro-intestinal media at 0.1%. Furthermore, an excess of $CaCl_2$ was added to obtain a concentration of 50 mM under SGF and FaSSIF conditions and 750 mM under FeSSIF conditions to mimic intestinal calcium concentrations and maintain cochleate structure. The cochleate suspensions, at an AmB concentration of 10 μg/mL, were first placed in SGF at 37 °C under shaking at a speed of 75 rpm for 1 h, after which an equivalent volume of either FaSSIF or FeSSIF medium at twice the desired final concentration was added.

The temperature and the stirring speed were maintained at 37 °C and 75 rpm respectively for 2 h. SGF aliquots of 0.3 mL were withdrawn at intervals and immediately neutralised with the same volume of buffer (0.11 M NaOH, 0.03 M NaH_2PO_4, 0.1% Tween 80) followed by centrifugation with an VWR Galaxy Mini Centrifuge C1413 8 (2000 × g, 10 min). After recovering the supernatant, 1 vol of MeOH was added followed by another centrifugation. FaSSIF and FeSSIF aliquots were filtered (0.2 μm PDVF syringe filter) and treated with 1 vol of MeOH followed by centrifugation. Supernatant from SGF, FaSSIF and FeSSIF samples were analysed for their AmB content by HPLC as described above.

2.12. Cell culture

Caco2 cells (passages 3–20 after thawing of cryo-preserved cells) were grown in DMEM supplemented with 20% FBS, 1% non-essential amino acids, 1% L-glutamine and 1% penicillin–streptomycin mixture and kept at 37 °C in 5% CO_2 and 95% humidity. Cells were washed with PBS and harvested with Trypsin-EDTA. Cells were cultured at a density of 15×10^3 cells/well onto 96-well cluster trays and allowed to grow for 24 h before cytotoxicity studies. For fluorescence confocal

microscopy studies, 5×10^4 cells were added to each Corning Transwell® insert (12 mm diameter, 0.4 μm pore size polyester membrane) and allowed to grow into monolayers for at least 21 days. For transport studies, 1.20×10^5 cells were added to each Corning Transwell® insert (24 mm diameter, 0.4 μm pore size polycarbonate membrane) for AmB permeability study and again grown for at least of 21 days. To verify the integrity of the monolayer the transepithelial electrical resistance (TEER) was measured using an EVOM2™ Epithelial Voltohmmeter with a STX2 electrode (Sarasota, USA) before and after each experiment. Furthermore, a marker of paracellular passage (FITC-dextran, 4.4 kDa) was also used periodically to check that tight junctions were maintained.

2.12.1. Cytotoxicity studies: MTT assay

Cell viability in the presence of cochleate formulations was studied using the MTT colorimetric method (Ménez et al., 2006b). Caco2 cells cultured in 96-well culture plate were exposed apically to increasing concentrations of AmB in the form of cochleates (0.1 μg/mL, 1 μg/mL, 10 μg/mL and 100 μg/mL of AmB) and incubated for 24 h. Unloaded cochleates, F0, were added at lipid concentrations equivalent to F0.5, the formulation with the lowest proportion of AmB and therefore the highest proportion of lipid. After 24 h of exposure, 20 μL of MTT solution (5 mg/mL in PBS) were added to each well and the plates were incubated at 37 °C for 2 h. The medium was removed and then 200 μL of DMSO was added to each well, and the plate was agitated until dissolution of the dark blue crystals. The optical density of the samples was measured at 570 nm using a multiwell-scanning spectrophotometer (LT-5000 MS, Labtech). The cytotoxicity of a control formulation without AmB was also evaluated, as was a suspension of AmB as the pharmaceutical formulation Fungizone®. Five replicate wells were used in each of triplicate experiments. The results are expressed as percentages of normalized mean control optical density. Treatment groups were compared using Student's two-tailed *t* test, with a P of $< 5\%$ being considered as significant.

2.12.1.1. Interaction of cochleates with Caco2 cells by confocal fluorescence microscopy. Cochleates labeled with 1,2-dioleoyl-*sn*-glycero-3-phosphoethanolamine-N-(lissamine rhodamine B sulfonyl) (ammonium salt) were used for the purpose of studying the interaction and internalization of cochleates by Caco2 cells that had been cultured for at least 21 days. Before the experiment, the confluence and the integrity of the monolayer was verified by measurement of TEER (values greater than 200 $\Omega.cm^2$) (Hubatsch et al., 2007) and cumulative transport values of FITC-Dextran 4.4 kDa after 4 h of incubation (~0.64 μg/mL) (Kowapradit et al., 2010). The Caco2 cells were incubated for 2 h with the Rhodamine-labeled cochleates (3 mg cochleates/ml equal to 40 μg/mL AmB) added to the upper compartment in HBSS pH 6.5. The medium in the lower compartment was HBSS at pH 7.4 supplemented with albumin at 4% (w/v). After incubation, the medium was removed and washed 3 times with PBS (Hubatsch et al., 2007). Cells were fixed with paraformaldehyde 4% for 15 min, washed three times with PBS and treated with 0.1% Triton X-100 for 10 min for permeabilization. Three washes of PBS were carried out followed by incubation with 50mMol NH_4Cl for 10 min. The inserts were then washed with PBS and treated with 1% BSA for 1 h. After removing the medium, the inserts were incubated with FITC-phalloidin (1/1000 in PBS 1% BSA) to label the cytoskeleton. After three washes with PBS, the filters bearing the cell monolayers were cut out of the supports and mounted on coverslips for examination by confocal microscopy with an inverted confocal laser scanning microscope TCS SP8 – gated STED Leica (Leica, Germany) equipped with a WLL Laser (495 nm excitation wavelength for FITC-phalloidin and 552 nm for rhodamine-nanoparticles). Green fluorescence emission was collected with a 505–550 nm wide emission slits and a 565–700 nm wide emission slits for the red signal under a sequential mode. Images were done with the Leica Application Suite X software (Version 3.5.5; Leica, Germany).

2.12.1.2. Uptake and transport of AmB by Caco2 cell monolayers. These experiments were performed on Caco2 cell monolayers that had been cultured for at least 21 days. The TEER was measured both before and after the experiment to ensure the integrity and the confluence of the monolayer in the presence of AmB-loaded cochleates. The cell monolayers were incubated for 6 h with the different cochleate formulations at a fixed AmB concentration of 100 μg/mL added to the upper compartment in HBSS pH 6.5. The medium in the lower compartment was HBSS at pH 7.4 containing 4% (w/v) albumin. At the end of the incubation period, the amount of AmB transported across the Caco2 monolayer was determined by recovering the solution from the lower compartment that was added to 2 volumes of acetonitrile and centrifuged (2000 × g, 10 min) to eliminate precipitated albumin. The excess solvent was evaporated under a nitrogen stream followed by freeze-drying for 24 h. Finally, a mixture of water/methanol (1/3) was added to dissolve the residue, obtaining a concentrated sample for analysis by HPLC as described above. In this case the limit of detection was 10 ng/mL and the limit of quantification was 25 ng/mL. The accumulation of AmB within the cell monolayers was also measured. The monolayers were rinsed five times with ice-cold PBS and solubilized with 1% Triton X-100 in water before adding to 3 volumes of methanol followed by centrifugation (2000 × g, 10 min). Finally, the supernatant was recovered to measure the AmB concentration by HPLC.

3. Results and discussion

3.1. Identification of phosphatidylserine species in Lipoid PSP70

After ion exchange, HPLC-MS of the Lipoid PSP70 revealed a large majority of phosphatidylserine. Phosphatidylcholine were also identified with a maximum content of 6% with respect to the total amount of phospholipids detected (see Supplementary Information, Figure S2). Further analysis revealed 11 different species of phosphatidylserine with different acyl chain lengths and degrees of unsaturation, as would be expected from a naturally occurring soy phospholipid (Table 1 and Figure S3). The acyl chains contained 16 or 18 carbon atoms, and were either saturated or with 1, 2 or 3 unsaturated bonds, with phosphatidylserine (18:2/18:2) being the most abundant, according to the peak heights. This means that the natural lipid is quite similar to DOPS (18:1/18:1) in terms of chain length and average level of unsaturation but is less homogenous. A 56 ± 7% recovery of phosphatidylserine was obtained after ion exchange. Therefore, as a negatively charged lipid

Table 1
Phosphatidylserine species composition of Lipoid PSP70 identified by MS^2 mass spectrometry. Where PS (AC1/AC2) denotes that AC1 is on one of the *sn*-1 carbon and AC2 is on the *sn*-2 carbon while PS (AC1-AC2) denotes that the position of the two acyl chains is unknown.

Observed ions $[M-H]^-$	PS Associated
756.4810	PS (16:0 – 18:3)
	PS (16:1 – 18:2)
758.4962	PS (16:0 – 18:2)
760.5083	PS (16:0 – 18:1)
780.4799	PS (18:3 – 18:2)
782.4950	PS (18:2/18:2) Majority
	PS (18:3 – 18:1)
784.5082	PS (18:2 – 18:1)
	PS (18:3 – 18:0)
786.5239	PS (18:0 – 18:2)
	PS (18:1 – 18:1)

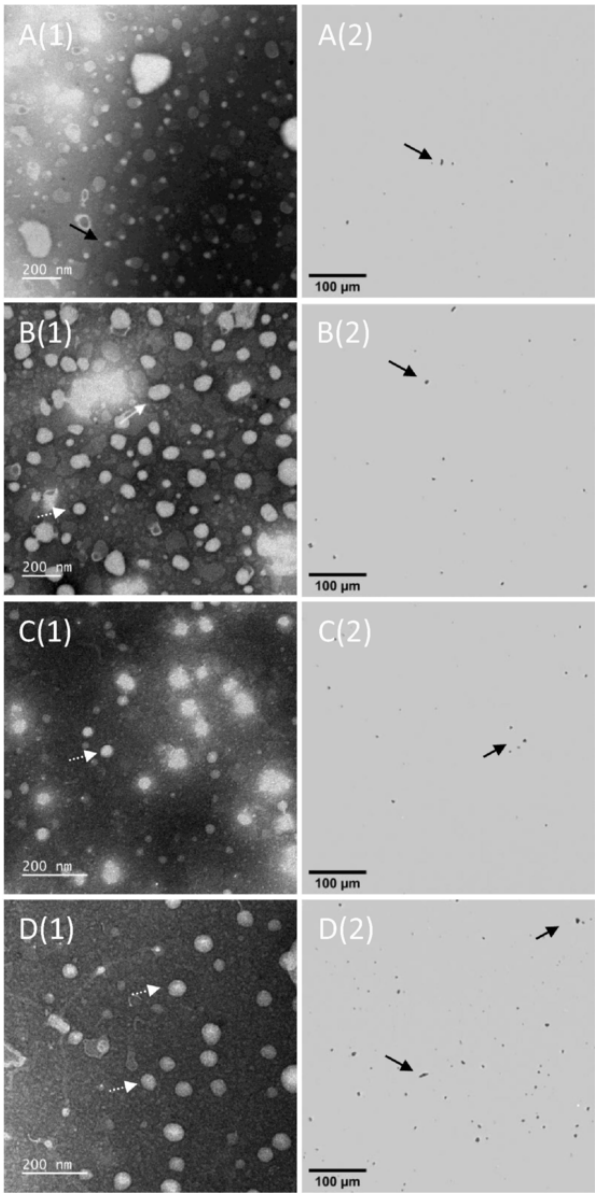

Fig. 1. AmB-Lipoid PSP70 cochleates observed by transmission electron (1) and optical microscopy (2). Formulation compositions are given in Materials and Methods. A: F0.5–9 Lipoid PSP70/2 cholesterol/0.06 vitamin E/0.5 AmB; B: F1 – 9 Lipoid PSP70/2 cholesterol/0.06 vitamin E/1 AmB; C: F2 – 9 Lipoid PSP70/2 cholesterol/0.06 vitamin E/2 AmB; D: F3 – 9 Lipoid PSP70/2 cholesterol/0.06 vitamin E/3 AmB.

with a high phosphatidylserine content, Lipoid PSP70 would be suitable for forming cochleates (Nagarsekar et al., 2017).

3.2. Morphology, size, polydispersity index and encapsulation efficiency

Cochleate structures are described as large, continuous lipid bilayer sheets rolled up into a rigid spiral, with no internal aqueous space (Zarif et al., 2000). To examine the structure of the formulations we studied them by TEM and morphogranulometry using an optical microscope. Fig. 1 corresponding to AmB-loaded cochleates obtained from Lipoid PSP70. Fig. A(1) shows precipitates mainly as cigar-shapes (black arrows) while B(1), C(1) and D(1) show objects with ovoid (white arrows) to spherical shapes (dotted white arrows), indicating an influence of the AmB content on the aggregation of liposomes and their subsequent precipitation as cochleates. Furthermore, the observed particles are in the nanometer range, in agreement with what would be expected by the hydrogel isolation method to obtain nanocochleates (Jin et al., 2000). Images A(2), B(2), C(2) and D(2) obtained by optical microscopy shows some larger cochleates, (black arrows), maybe due to the presence of other lipid species in the naturally occurring phospholipid or to the variability of the acyl chains of the phosphatidylserine; leading to less ordered structure, but which could also be caused by calcium ion excess, a serious drawback reported in the fabrication of cochleates where excess calcium can provoke fusion between cochleates (Bozó et al., 2017).

The values obtained for zeta potential (Table 2) also indirectly confirm the bridging of the phosphatidylserine bilayers by calcium. While the zeta potential of the liposomes was highly negative (-43 mV or more), the values recorded under the same conditions for the resulting cochleates were between −9 and −16 mV, showing the neutralization of the charge on the phosphatidylserine headgroup by calcium ions.

Unloaded and AmB-loaded cochleates from Lipoid PSP70 were characterized in terms of size and homogeneity by dynamic light scattering. In Table 2 the cochleate dimensions were 221, 469, 470, 626, 752 nm, confirming the nanometric scale found by electronic microscopy. The cochleate dimensions appeared to increase with the proportion of AmB, although the size of the liposomes used to prepare them was always calibrated on 100 nm pore size membranes and was between 71 and 90 nm. However, dynamic light scattering is not the ideal method for determining the average size of anisotropic particles such as cochleates because the algorithms used to deduce size from diffusion constants assume that the particles are spherical. The high PdI that were obtained are partly a reflection of this limitation but are also in agreement with the observations from microscopic techniques. Heterogeneous dispersions are frequently observed for nanocochleates (Nagarsekar et al., 2017). Since the present formulation is intended for oral use, small and monodisperse particles are not as high a requirement as they would be for parenteral administration. However, smaller particles are desirable to allow better drug release and it is necessary that the fabrication process be reproducible; thus, the procedure needs to be further improved before *in-vivo* use. On the other hand, increasing val-

Table 2
Physical and chemical characterization of AmB-loaded liposomes and cochleates.

Parameter Formulation	Size (liposomes)		Size (cochleates)		Zeta Potential (mV)		AmB (µg/mg cochleate)	Encapsulation Efficiency (%)
	D_h (nm)	PdI	D_h (nm)	PdI	as liposomes	as cochleates		
F0	90	0.160	221	1.000	−47.8	−13.5	-----	-----
F0.5	71	0.220	469	1.000	−48.6	−12.2	57 ± 3	64 ± 4%
F1	78	0.280	470	1.000	−59.2	−10.1	107 ± 5	62 ± 3%
F2	83	0.240	626	0.668	−48.9	−9.15	193 ± 4	56 ± 1%
F3	71	0.190	752	0.634	−43.8	−15.9	264 ± 5	65 ± 1%

D_h: Equivalent hydrodynamic diameter; PdI: Polydispersity index. Values expressed as mean ± SD (n = 3)
Cochleate compositions are as follows: F0.5: 9 Lipoid PSP70/2 cholesterol/0.06 vitamin E/0.5 AmB; F1: 9 Lipoid PSP70/2 cholesterol/0.06 vitamin E/1 AmB; F2: 9 Lipoid PSP70/2 cholesterol/0.06 vitamin E/2 AmB; F3: 9 Lipoid PSP70/2 cholesterol/0.06 vitamin E/3 AmB.

ues of the zeta potential observed in all formulations after the addition of calcium ions shows the complexation of the negative charge on the phospholipid that triggers cochleate formation. Finally, the AmB entrapment efficiency of more than 55% demonstrates the efficiency of the cochleates from Lipoid PSP70 to encapsulate AmB within the lamellar phase. Furthermore, increasing the proportion of AmB in the formulation from 0.5 to 3 mol did not reduce significantly the encapsulation efficiency (~64, 62, 56 and 65%). Therefore, the results show that it is possible to increase the proportion of AmB stably encapsulated in the cochleates above that described in the literature (Pham et al., 2013, Zarif et al., 2000).

3.3. Small-angle X-ray scattering

The SAXS patterns obtained (Fig. 2 and Table S4) clearly show the transformation of the negatively charged fluid-phase Lipoid PSP70 liquid crystalline vesicular membranes into densely packed multilamellar structures (Lipoid PSP70/Ca^{2+} or Lipoid PSP70/cholesterol/ Ca^{2+}) stabilized by electrostatic interactions with the divalent cations. The formation of salt bridges between the lamellae led to dehydration of the multilamellar phospholipid organization, which was associated with the emergence of well-defined Bragg peaks in the SAXS patterns. The possibility of identifying the formation of cochleate structures by SAXS has been examined for other lipid compositions in the literature (Nagarsekar et al., 2016; Hui et al., 1983). Depending on the ratio between the components in the self-assembled systems, the decrease of the repeated distances (d) of the multilamellar lipid vesicles (MLV) upon the addition of a bridging agent may correspond to either pure cochleate system or to a coexistence of cochleates and the multilamellar vesicles that existed before addition of the bridging agent.

Fig. 2 and Table S4 show the SAXS results obtained as a function of the lipid compositions Lipoid PSP70 with and without calcium and Lipoid PSP70/cholesterol with different proportions of AmB in the presence of calcium. Additional results are presented in the Supporting Information for varying contents of cholesterol in the mixtures with a constant proportion of AmB (Figure S1). The structural transition between the different aggregation states of the lipid bilayers in the Lipoid PSP70-based formulations is remarkable. Fig. 2A presents the SAXS pattern of a hydrated lamellar structure (Lipoid PSP70 MLV) with a repeat distance of $d = 57.2$ Å. The observed peak intensity and full width at half maximum (FWHM) indicate the formation of onion-like multilamellar membranes with no dense packing between the lamellae. In contrast, the appearance of narrow Bragg peaks upon the addition of calcium cations to the Lipoid PSP70 MLV demonstrates the condensation of the lamellae into a layered structure with increased packing order. As can be observed in Fig. 2B (Lipoid PSP70 cochleates), the SAXS plot shows an intense first-order peak corresponding to a repeat interlamellar distance of 49.1 Å as well as second and third order reflections characterizing the multilamellar organization.

These repeat spacings indicate that the cochleates are comprised of dehydrated multilamellar phase assemblies. In this arrangement, the lipid molecules form a well-packed bilayer structure with a multibilayer periodicity, in which the phospholipid head groups are suggested to be oriented parallel to the bilayer plane and the acyl chains are organized in a more confined space (Garidel et al., 2001). The intermembrane space is reduced owing to the attractive interactions between the phosphoserine headgroups and the Ca^{2+} ions that cause considerable changes of the water layer thickness (*i.e.* dehydration). Within the induced topology of this kind of lipid aggregates, Ca^{2+} ions gradually replace water of hydration from the phosphate group forming a tight, anhydrous Ca-lipid chelate. It has been suggested that decreasing in the thickness of the water layer is due to the formation of bridges between the two bilayers (Hauser et al., 1977).

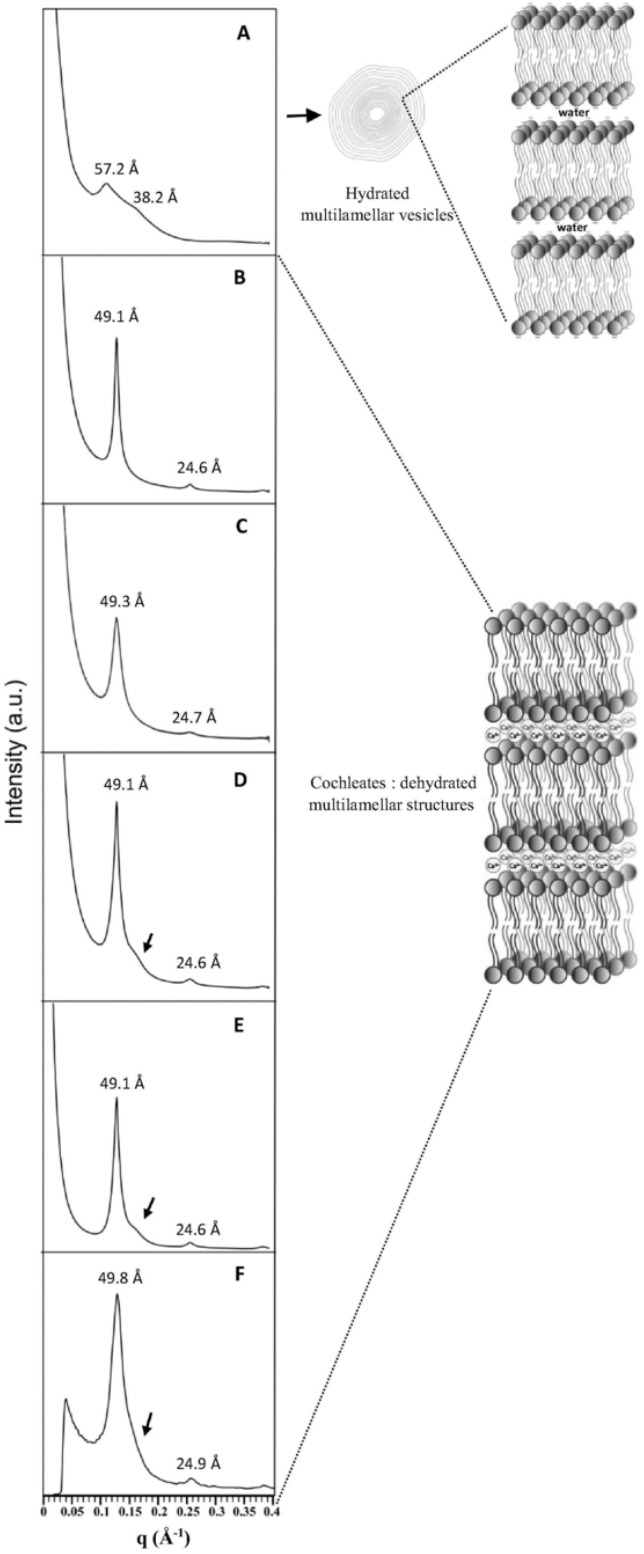

Fig. 2. Small-angle X-ray scattering (SAXS) spectra of Lipoid PSP70 in various formulations (compositions are expressed in molar proportions). A: Lipoid PSP70 as multilamellar vesicles; B: Lipoid PSP70 as cochleates; C: 9 Lipoid PSP70 /2 Cholesterol/ 0.5 AmB as cochleates (F0.5); D: 9 Lipoid PSP70 /2 Cholesterol /1 AmB as cochleates (F1); E: 9 Lipoid PSP70 /2 Cholesterol /2 AmB as cochleates (F2); F: 9 Lipoid PSP70 /2 Cholesterol /3 AmB as cochleates (F3).

Fig. 2C to F demonstrates the formation of cochleates with increasing proportions of the incorporated drug AmB (F0.5, F1, F2 and F3). The cochleates formulated at a constant molar fraction of cholesterol in the bilayers were characterized with a similar interlamellar distance as that for Lipoid PSP70 alone (Fig. 2B). In Fig. 2C, the SAXS pattern obtained at a 9/2/0.5 ratio of phospholipid, cholesterol and AmB, the profile was similar to Fig. 2B, indicating that the dehydrated lamellar phase was able to accommodate AmB.

As a comparison, formulations made with the synthetic phosphatidylserine DOPS were also examined. Supplementary Fig. 4A shows cochleates made from DOPS and cholesterol in 9/1 M proportions that demonstrate a sharp first-order Bragg peak at 51.7 Å, while a formulation containing DOPS, cholesterol and AmB in 9/1/0.5 M proportions displayed a peak at 51.2 Å (Supplementary Fig. 4B). Therefore, the structures formed by Lipoid PSP70 are similar to those formed by the synthetic phospholipid that has most often been used to form cochleates.

The SAXS patterns shown in Supplementary Fig. 1 show that the position of the first-order Bragg peak was not affected by the proportion of cholesterol, at a constant AmB proportion. However, with very high cholesterol content, a small addition peak appeared (indicated by the black arrow in Figure S1E). Therefore, cholesterol contents up to a 9/4 M ratio with phospholipid does not hamper cochleate formation. However, when the proportion of AmB in Lipoid PSP70 cochleates is increased, a small additional peak can be seen (indicated by arrows in Fig. 2D, E and F), probably due to the formation of a second phase.

Preliminary studies with wide-angle X-ray diffraction (WAXS) did not show any well-defined peaks and could not be interpreted. This was due to the heterogenous nature of the phospholipid as well as the presence of cholesterol, so that no ordered structure could be seen in the plane of the bilayer.

In conclusion, the SAXS results have confirmed the ability of Lipoid PSP70 to form dehydrated multilayer assemblies on interaction with calcium ions in the same way as the synthetic DOPS. They have also defined the limits for the inclusion of cholesterol and AmB in the structures. Complementary studies of stability in the gastric environment and the state of aggregation of AmB will help to clarify whether the appearance of a new phase in the presence of higher proportions of AmB can alter the ability of the cochleates to deliver AmB effectively and to reduce its toxicity.

3.4. Circular dichroism and UV–visible spectroscopy

The AmB molecule has a particular cyclic structure with seven conjugated double bonds which give rise to intense absorption peaks between 250 and 450 nm. Its spectral properties depend on whether the molecule is in monomeric form, aggregated or complexed with other molecules. In consequence, electronic absorption and CD spectroscopy are useful tools for studying the organization of AmB within formulations (Barwicz et al., 1993; Gaboriau et al., 1997). This is important because the pharmacological activity and the toxic side effects of AmB are strongly dependent on its molecular organization (Barwicz et al., 1992). Therefore, the aggregation state of AmB within the Lipoid PSP70 formulations was investigated. However, samples for UV and CD spectroscopy must be homogeneous and free from highly light-scattering particles to prevent interference (Kelly and Price, 2000). Since the final cochleates do not fulfil these criteria, the measurements were carried out on the cochleates treated with 0.05 M EDTA to reconvert them into liposomes (Pham et al., 2014). Unloaded cochleates treated in the same way were used as blanks.

In Fig. 3A, the UV–visible spectrum corresponding to AmB in methanol, shows a small band at 344 nm and pronounced bands at 365, 385 and 406 nm that correspond to the profile of AmB in the monomeric state. On the other hand, for the AmB diluted in water from a high concentration in DMSO there is a broad intense band around 342 nm, in addition to other bands of low intensity around 368, 387 and 420 nm. All these bands are characteristic of the aggregated state of AmB (Pham et al., 2014). Fig. 3A also shows the UV–visible spectrum of AmB-loaded cochleates in which four bands appear at 327 nm, 367 nm, 389 nm, and 415 nm for the F0.5 and F1 formulations and 325 nm, 367 nm, 389 nm, and 415 nm for the F2 and F3 formulations. These spectra differ from that of AmB in the aggregated state, suggesting that a part of the AmB in these formulations is maintained in its monomeric form. The band at 415 nm indicates a complexed form of AmB.

The CD spectrum of the aggregated form of AmB is known to display a very intense dichroic doublet with both positive and negative bands (Pham et al., 2014, Shervani et al., 1996, Barwicz et al., 2002). In Fig. 3B, the CD spectrum showing AmB diluted in water, the doublet was centered at 334 nm and the negative bands were detected at 370 nm, 394 nm and 424 nm. On the other hand, the monomeric form of AmB in methanol yields a CD spectrum with three weak positive bands at 360 nm, 382 nm, 405 nm, as observed by Pham et al. (2014). The CD spectra of all AmB-loaded cochleate formulations show a much lower intensity of both the positive band and the negative bands compared with AmB in water. Taken together, these findings indicate that some AmB in the formulations is present in the monomeric form. However, the appearance of a strong positive band at 327 nm in the UV–visible spectrum (for F0.5 and F1) or at 325 nm (for F2 and F3) leads to a change in the intense dichroic doublet from 345 nm to 329 nm (or 327 nm), a decrease in intensity of the negative bands and the appearance of a positive band at 425 nm in the CD spectrum. Thus, the molecular state is related to the proportion of AmB in the preparation. These results are characteristic of the interaction of AmB with other components such as cholesterol and/or phospholipid present in the formulation (complexed AmB) (Pham et al., 2014). This suggests that AmB-cochleate formulations contain AmB in both its monomeric and complexed forms and that the complexed form becomes more prevalent as the proportion of AmB increases. These results led us to expect the cochleate formulation to be less toxic than the pharmaceutical form (Fungizone®) by avoiding or reducing the self-associated form (aggregated state) (Barwicz et al, 1992).

3.5. Stability study of AmB-cochleates in SGF medium

Table 3 clearly shows that free AmB, added as a concentrated solution in DMSO, was unstable when exposed to SGF medium, since only about 17% was recovered after 2 h of exposure. In contrast, all formulations of AmB as cochleates show a significant improvement with approximately 81, 73 and 77% recovery for the formulations F0.5, F1 and F2 respectively, while lower protection was observed for the cochleate formulation F3 with the highest proportion of AmB, where the recovery was 64%. Most of the degradation was observed during the first hour, while only a small additional loss during the second hour. Part of the degradation observed during the first hour could be due to the small percentage of AmB that was not tightly associated with the cochleates (see Section 2.7) and there is probably also some AmB release from the outer layer of the cochleate structure. The higher susceptibility of the AmB in the formulation containing the highest molar proportion (F3) may be due to the presence of a small amount of a different structure, as indicated by the shoulder in the SAXS pattern in Fig. 2F, that does not afford as much protection as the cochleate phase.

3.6. In-vitro release study

The profiles in Fig. 4 show a release of approximately 10%, 6%, 10%, 5% of the encapsulated AmB after incubation for 1 h under gastric conditions and 3%, 4%, 5% and 2% after a further 2 h of incubation in FaSSIF conditions for formulations F0.5, F1, F2 and F3 respectively;

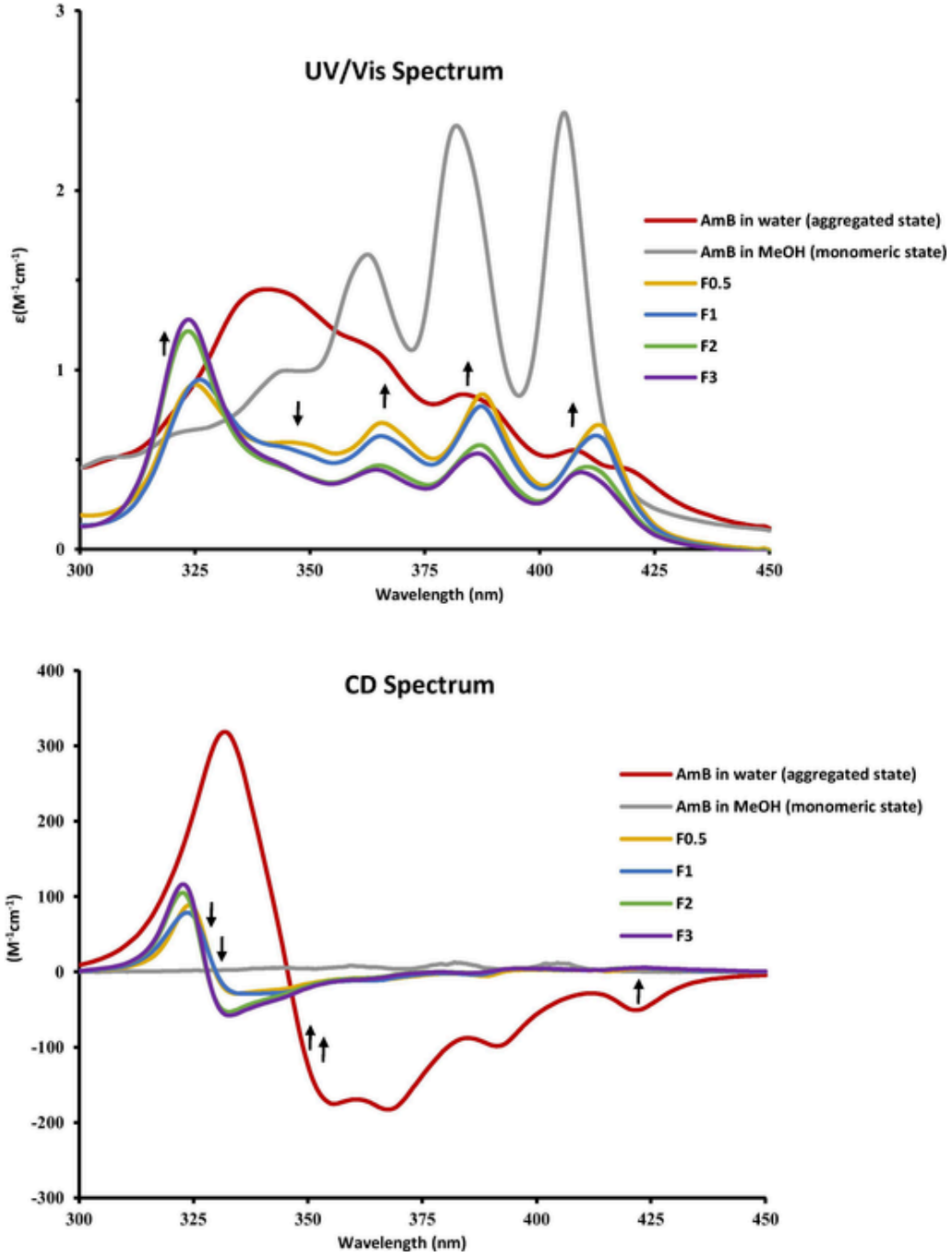

Fig. 3. UV spectra (ε M^{-1} cm^{-1}) (A) and CD spectra (Δε M^{-1} cm^{-1}) (B) of AmB in methanol, in water, and in cochleate formulations treated with 0.05 M EDTA. F0.5: 9 Lipoid PSP70/2 cholesterol/0.06 vitamin E/0.5 AmB; F1: 9 Lipoid PSP70/2 cholesterol/0.06 vitamin E/1 AmB; F2: 9 Lipoid PSP70/2 cholesterol/0.06 vitamin E/2 AmB; F3: 9 Lipoid PSP70/2 cholesterol/0.06 vitamin E/3 AmB. The arrows indicate changes in the spectra of the cochleates compared with that of AmB in water.

however significant amounts of release of 70%, 56%, 49% and 75% were observed when the second incubation was in FeSSIF intestinal conditions. These values indicate the ability of the cochleates to retain AmB under SGF and fasting conditions (FaSSIF) but to release it in presence of a high concentration of bile salts (FeSSIF). It is known that bile salts form mixed micelles with lipids and disrupt lipid-based drug delivery systems (Andrieux et al. 2009) and similar behavior was observed by Pham et al. (2014) for DOPS-based cochleates. The degree of release in FeSSIF differed between the formulations; the highest release being obtained for the formulation with the lowest molar proportion of AmB (F0.5) and for that with the highest (F3). This could be explained by two phenomena acting at the same time. One is the strength of the association of AmB with the lipids in cochleates which would be lowest with the highest proportion of AmB to lipid, as already shown by the reduced protection of AmB in formulation F3 (Table 3). The other might be the total surface area developed by the formulation. Since the experiments were carried out at a fixed concentration of AmB, for F0.5 a large number of particles were present, giving a higher surface area to interact with bile salts. Whatever the release from individual formulations, it is clear from the results that AmB release is greatly increased in "fed" conditions. It is interesting to note that mixed lipid-bile salt micelles have been shown to promote the intestinal absorption of AmB (Dangi et al., 1998).

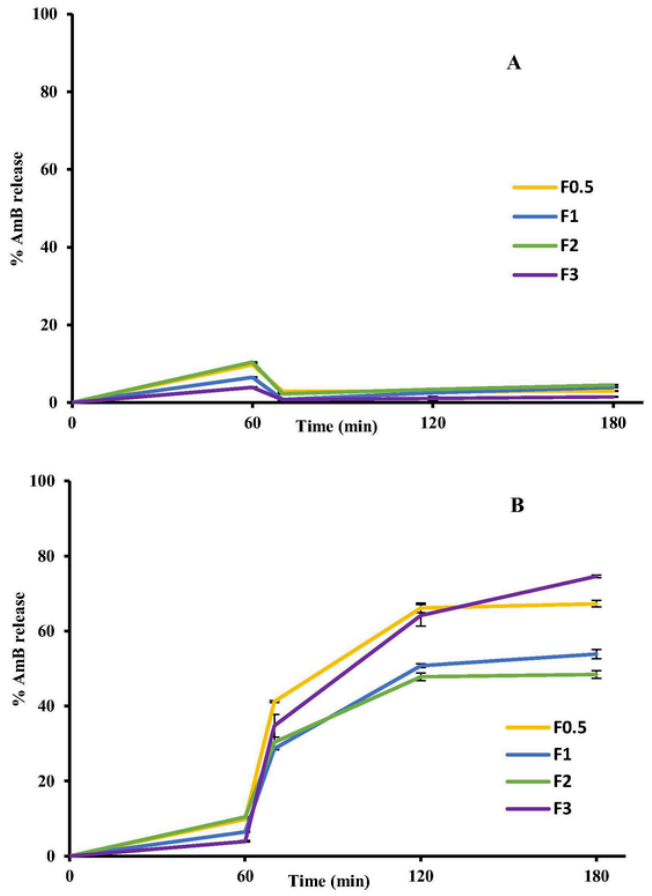

Fig. 4. Release profiles of AmB from different formulations in synthetic gastric fluid for 1 h followed by (A) fasted state synthetic intestinal medium (FaSSIF) and (B) fed state synthetic intestinal medium (FeSSIF) for a further 2 h. The initial AmB concentration was 10 μg/mL. Values are expressed as mean ± SD (n = 3) of three determinations of AmB content in samples measured by HPLC and expressed as a percentage of the original amount. F0.5: 9 Lipoid PSP70/2 cholesterol/0.06 vitamin E/0.5 AmB; F1: 9 Lipoid PSP70/2 cholesterol/0.06 vitamin E/1 AmB; F2: 9 Lipoid PSP70/2 cholesterol/0.06 vitamin E/2 AmB; F3: 9 Lipoid PSP70/2 cholesterol/0.06 vitamin E/3 AmB.

Table 3
AmB stability in synthetic gastric medium (SGF). Values are the percentage of intact AmB recovered, mean ± SD for 3 determinations.

Formulation	AmB (%) after 1 h	AmB (%) after 2 h
AmB in DMSO	37 ± 1	17 ± 1
F0.5	85 ± 2	81 ± 1
F1	81 ± 1	73 ± 2
F2	88 ± 1	77 ± 2
F3	72 ± 2	64 ± 4

Cochleate compositions are as follows: F0.5: 9 Lipoid PSP70/2 cholesterol/0.01 vitamin E/0.5 AmB; F1: 9 Lipoid PSP70/2 cholesterol/0.01 vitamin E/1 AmB; F2: 9 Lipoid PSP70/2 cholesterol/0.01 vitamin E/2 AmB; F3: 9 Lipoid PSP70/2 cholesterol/0.01 vitamin E/3 AmB.

3.7. Effects of AmB-loaded cochleates on Caco2 cell viability

As shown in Fig. 5, none of the formulations tested reduced Caco2 viability, as determined by MTT reduction, by more than 30% during 24 h of exposure. A slight increase in Caco2 cell viability was observed with the F0 and F0.5 formulations at 100 μg/mL after 24 h of exposure, probably due to the higher lipid load that favors cell growth (Hossain et al., 2006). There were no significant differences between F0.5, the formulation with the lowest proportion of AmB and F0 at the same lipid concentrations without AmB. However, for the formulations with higher AmB proportions, F1, F2 and F3, some significant reductions of viability were observed after exposure to at 100 μg/mL of AmB when compared to untreated controls were observed, especially at the highest AmB concentration ($P < 0.05$, as indicated on Fig. 5). However, the viability was never lower than 80% with the cochleate formulations, whatever the concentration tested. The pharmaceutical formulation, Fungizone® also reduced viability compared to untreated controls at concentration of 1 μg/mL and higher and was slightly more toxic than the cochleate formulations.

These results were confirmed by measurements of transepithelial electrical resistance, as shown in Table 4. Caco2 cell monolayers after at least 21 days of culture were incubated for 4 h with AmB at 100 μg/mL as different formulations. The pharmaceutical formulation Fungizone® reduced the TEER to 7% of its original value over this period. The cochleate formulations also reduced the TEER, to between 57 and 72% of the starting value, but the resistance remained higher than 200 $\Omega.cm^2$ that is considered to indicate intact monolayers (Hubatsch et al., 2007).

These observations are consistent with those obtained from circular dichroism that the association with lipids in the cochleates can reduce the proportion of toxic forms of AmB. They are also in agreement with many other studies that demonstrate reduced toxicity of lipid-based formulations of AmB compared with Fungizone® in many different cells types; for example in alveolar epithelial cells (Menotti et al., 2017).

3.8. Interactions of Rhodamine-labeled cochleates with Caco2 cells

The interaction of the cochleates with the intestinal cells was followed by labeling unloaded cochleates with Rho-PE while the cytoskeleton of the cells was labeled with FITC-phalloidin. In Fig. 6A1 and B1, the image in the fluorescein channel shows the typical Caco2 cell surface. The rhodamine channel in Figure A2, after exposure of the cells to Rho-PE as micelles in DMSO, shows few fluorescent objects while in Figure B2 after exposure to Rho-PE as cochleates, there is a considerable fluorescence signal, indicating accumulation of the Lipoid PSP70 cochleates on the cell surface. When images were recorded at the level of the cell interior (Fig. 6C and D), the fluorescein channel again showed the confluent Caco2 cells (Fig. 6C1 and D1), while the rhodamine channel showed very low fluorescence in the case of Rho-PE-DMSO micelles (Fig. 6C2) whereas the fluorescence signal from Rho-PE-cochleates Fig. 6(D2) was slightly higher.

3.9. Uptake and transport of AmB by Caco2 cell monolayers

The TEER values were unchanged after 6 h of incubation contact with AmB-loaded cochleates, confirming the MTT results showing that the drug in cochleate form was not highly toxic to Caco2 cells. Table 5 shows that the accumulation of AmB within the cells depended on the proportion of AmB in the cochleates, although the same amount of AmB was added in each case. For the formulations F0.5, F1 and F2, the percentage of added AmB recovered from the cells increased with the proportion of AmB, reaching almost 50% with the cochleates composed of Lipoid PSP70, cholesterol and AmB in 9/2/2 M proportions. However, the percentage captured decreased when the proportions were 9/2/3 (F3). The amount of AmB measured within the cell monolayer was between 34 and 71 μg.

A similar relationship with AmB proportion in the cochleates was seen when the amount that had been transported across the monolayer was considered. However, the percentage of added AmB that reached the baso-lateral compartment was very low, with a maximum of 0.07% with the formulation F2, corresponding to a concentration of 103 ng/mL, but remained above the limit of quantification of the HPLC method of 25 ng/mL . Taken with the results from confocal mi-

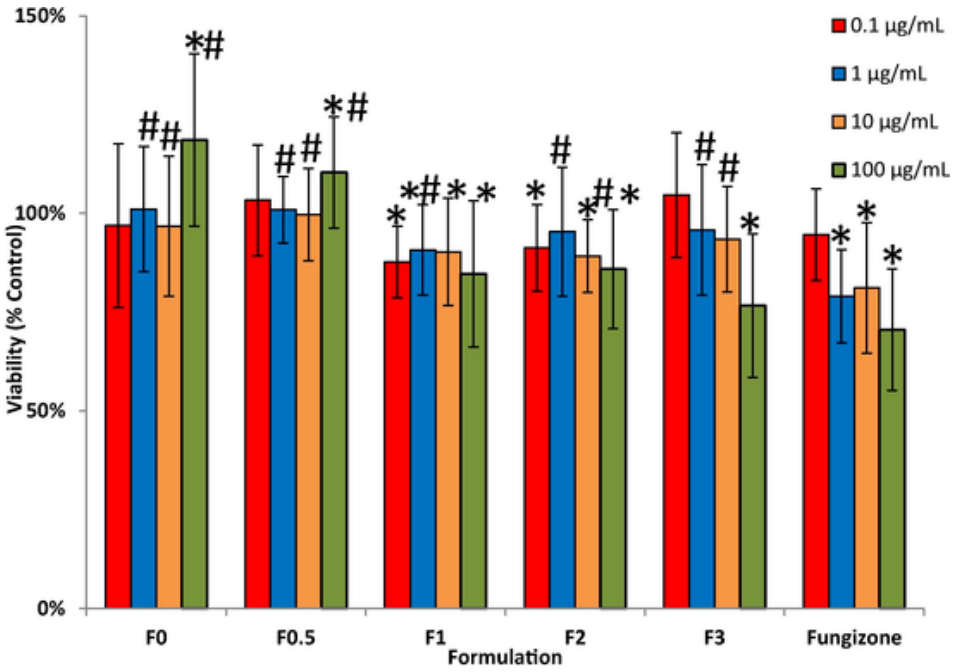

Fig. 5. Cytotoxic effects of AmB-loaded cochleates on Caco-2 cell monolayers after 24 h as a function of concentration, determined by MTT reduction. Values are expressed as percentages of untreated controls, mean ± SD of three experiments. * $P < 0.05$ for comparison with untreated control, # $P < 0.05$ for comparison with Fungizone at the same concentration, Student's unpaired two-tailed *t* test. F0.5: 9 Lipoid PSP70/2 cholesterol/0.06 vitamin E/0.5 AmB; F1: 9 Lipoid PSP70/2 cholesterol/0.06 vitamin E/1 AmB; F2: 9 Lipoid PSP70/2 cholesterol/0.06 vitamin E/2 AmB; F3: 9 Lipoid PSP70/2 cholesterol/0.06 vitamin E/3 AmB.

Table 4
Transepithelial electrical resistance (TEER) of Caco2 monolayers cultivated on inserts for at least 21 days before and after addition of 100 µg/mL of Amphotericin B in various cochleate formulations for 4 h of incubation. Values are expressed as mean ± SD of measurements from 3 inserts.

Formulation	TEER (Ω cm^2)	
	Before incubation	After incubation
AmB-Fungizone	486 ± 8	34 ± 3
F0.5	435 ± 5	249 ± 8
F1	440 ± 10	317 ± 10
F2	454 ± 7	310 ± 30
F3	452 ± 10	322 ± 20

Cochleate compositions are as follows: F0.5: 9 Lipoid PSP70/2 cholesterol/0.01 vitamin E/0.5 AmB; F1: 9 Lipoid PSP70/2 cholesterol/0.01 vitamin E/1 AmB; F2: 9 Lipoid PSP70/2 cholesterol/0.01 vitamin E/2 AmB; F3: 9 Lipoid PSP70/2 cholesterol/0.01 vitamin E/3 AmB.

croscopy, this suggests that the cochleates can be adsorbed onto the cell surface, followed by fusion and AmB transfer into the cell membranes, to be released later. An increase in the proportion of AmB could favor transfer, but at the highest proportion of AmB (F3) the lower proportion of phosphatidylserine may decrease the ability of the cochleates to fuse with cell membranes. However, it should be taken into account that Caco2 cells do not produce mucus and this could influence cochleate adherence *in vivo*. On one hand, the mucus could contribute to trapping cochleates on the surface of the epithelium; on the other hand, the large size of the cochleates could hamper their diffusion through the mucus later to the cell surface.

These results are consistent with the hypothesis of Zarif et al. (2000) that cochleate structures could improve the bioavailability of drugs by means of adhesion of the particles to the intestinal epithelium followed by fusion and incorporation of phosphatidylserine into the cell membrane to later release the encapsulated drug. Fig. 7 shows a schematic representation of this hypothesis.

After absorption through the intestinal epithelium AmB would be expected to bind to plasma lipoproteins (Wasan et al., 1998) and be carried to the liver via the hepatic portal vein. This "first-pass effect" is often a disadvantage for orally administered drugs but in the case of leishmaniasis treatment it is an advantage because the liver is the main organ harboring the parasites. As pointed out in a review by Serrano and Lalatsar (2017), plasma concentrations after oral administration of AmB formulations are not necessarily the best indication of efficacy; organ concentrations are also important. Thus, although the cochleate formulations that have been tested *in vivo* so far do not lead to high plasma concentrations, they can produce high concentrations in the liver, spleen and lungs. Interestingly, organ concentrations were found to be higher in mice infected with *Candida albicans* than in healthy animals (Mannino and Perlin, 2015).

The administration of cochleates containing AmB in models of fungal infection in mice also showed lower toxicity than Fungizone® (reviewed by Aigner and Lass-Flörl, 2020). Furthermore, in clinical trials, AmB-loaded cochleates were well tolerated in healthy volunteers and no serious side effects were observed in patients with fungal infections in phase II trials (Aigner and Lass-Flörl, 2020). We could therefore expect that our system, with similar physicochemical properties, would display similar *in-vivo* efficacy and tolerability in the case of leishmaniasis. This will be the subject of future investigation.

4. Conclusions

The study shows that it is possible to prepare cochleates containing AmB from an inexpensive and biocompatible naturally occurring phospholipid, Lipoid PSP70, while retaining the morphology, internal structure described for cochleates prepared from more costly synthetic phospholipids such as DOPS. Synchrotron SAXS experiments gave direct evidence the supramolecular organization of the multicomponent cochleate assemblies loaded with AmB. Furthermore, the entrapment efficiency, low toxicity, improved gastric stability and delayed *in-vitro* release of AmB from loaded cochleates were also promising for the oral administration. The formulation F2 (9 Lipoid PSP70/2 cholesterol/0.06

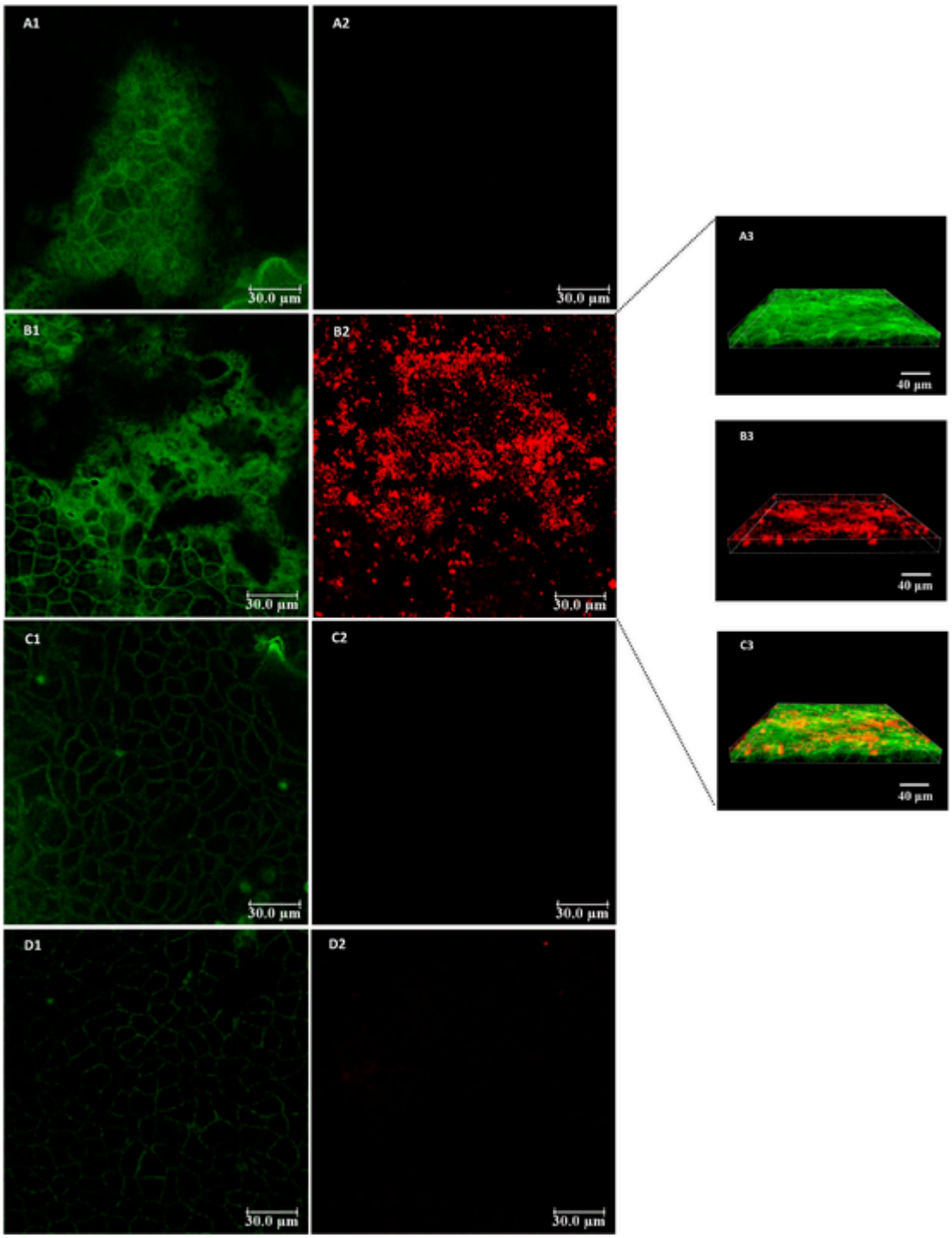

Fig. 6. Confocal microscopy images of Caco2 cells taken at the cell surface (A and B) and in the cell interior (C and D). The cytoskeleton was labeled with phalliodin-FITC (green fluorescence) and the cochleates with rhodamine (red fluorescence) Fluorescein emission (1) and Rhodamine emission (2) after exposure for 2 h to Rhodamine-PE micelles (Controls, A and C) and Rhodamine-PE cocheates (9 Lipoid PSP70 /2 cholesterol /0.018 Rho-PE/ 0.06 vitamin E, B and D). In images on the left are 3-D reconstruction showing the possible absorption and fusion of the cochleates on the cell membrane: A3: Fluorescein emission (cytoskeleton); B3: Rhodamine emission (cochleates); C3 overlay.

vitamin E/2 AmB) contains a high proportion of AmB compared with cochleate formulations previously described in the literature. Studies on Caco2 cell monolayers have thrown light on the possible mechanism of action of these drug delivery systems: incorporation of phosphatidylserine into the cell membrane and the subsequent release of the drug into the cell. The use of a naturally occurring phosphatidylserine from soy that is considerably less expensive than the synthetic phospholipid DOPS means that further experiments can be carried out at reduced cost. These should allow better understanding of cochleates, such as their uptake mechanism and to investigate the improved bioavailability of AmB and activity *in-vivo* after oral administration. The lower raw material cost also allows these systems to be considered for use in developing countries. In this respect, another important point is the ability of cochleates to undergo freeze-drying and reconstitution without any cryoprotector being necessary. All these factors suggest that

Table 5
Uptake of AmB into Caco-2 cell monolayers grown on inserts and passage to the lower compartment. Inserts were incubated for 6 h with 100 μg/mL AmB in various cochleate formulations added to the upper compartment. Results are expressed as the percentage of added AmB found into cell monolayer and in the lower compartment as the mean ± SD of 3 inserts.

Formulation	AmB in the cell monolayer (%)	AmB in the lower compartment (%)
F0.5	23 ± 3	Non-detectable
F1	31 ± 2	0.019 ± 0.003
F2	47 ± 2	0.069 ± 0.008
F3	43 ± 3	0.035 ± 0.011

Cochleate compositions are as follows: F0.5: 9 Lipoid PSP70/2 cholesterol/0.01 vitamin E/0.5 AmB; F1: 9 Lipoid PSP70/2 cholesterol/0.01 vitamin E/1 AmB; F2: 9 Lipoid PSP70/2 cholesterol/0.01 vitamin E/2 AmB; F3: 9 Lipoid PSP70/2 cholesterol/0.01 vitamin E/3 AmB.

AmB-loaded cochleates would be a promising tool for oral therapy of leishmaniasis in the regions where it is endemic.

CRediT authorship contribution statement

Antonio Lipa-Castro: Investigation, Writing - original draft. **Valérie Nicolas:** Resources, Formal analysis, Writing - original draft. **Angelina Angelova:** Investigation, Methodology, Formal analysis, Writing - review & editing. **Ghozlene Mekhloufi:** Investigation, Formal analysis, Writing - review & editing. **Bastien Prost:** Investigation, Methodology, Formal analysis. **Monique Chéron:** Investigation, Formal analysis. **Vincent Faivre:** Investigation, Methodology, Formal analysis, Writing - review & editing. **Gillian Barratt:** Conceptualization, Supervision, Writing - original draft, Writing - review & editing.

Declaration of Competing Interest

The authors declare that they have no known competing financial interests or personal relationships that could have appeared to influence the work reported in this paper.

Acknowledgements

A. L-C. received a Ph.D. grant from FONDECYT, Peru. A.A. acknowledges the allocation of beam time at Synchrotron SOLEIL (Saint Aubin, France) through the project 20191836 and the scientific and technical support of Dr. T. Bizien at the SWING beamline. The authors would like to thank Audrey Solgadi (Université Paris-Saclay, Inserm, CNRS, Ingénierie et Plateformes au Service de l'Innovation Thérapeutique) for help with the analysis of phospholipids in Lipoid PSP70; Claire Boulogne and Cynthia Gillet (Imagerie-Gif) for help with electron microscopy; Claire Gueutin (Institut Galien Paris-Saclay) for help with the analysis of AmB. Nicolas Huang and Baptiste Robin (Institut Galien Paris-Saclay) for help with morphogranulometry. We thank Jean-Jacques Vachon (Institut Galien Paris-Saclay) for help with X-ray diffraction experiments and also Claudie Bourgaux (Institut Galien Paris-Saclay) for performing additional SAXS experiments. We are grateful to Christina Sizun (Université Paris-Saclay, CNRS, Institut de Chimie des Substances Naturelles, UPR 2301) for preliminary studies with circular dichroism and François-Xavier Legrand for useful discussions. We thank Joelle Salameh (Mécanismes cellulaires et moléculaires d'adaptation au stress et cancérogénèse, Faculté de Pharmacie, Université Paris-Saclay) for the gift of FITC-phalloidin.

This work did not receive any specific grant from funding agencies in the public, commercial or not-for-profit sectors for running costs.

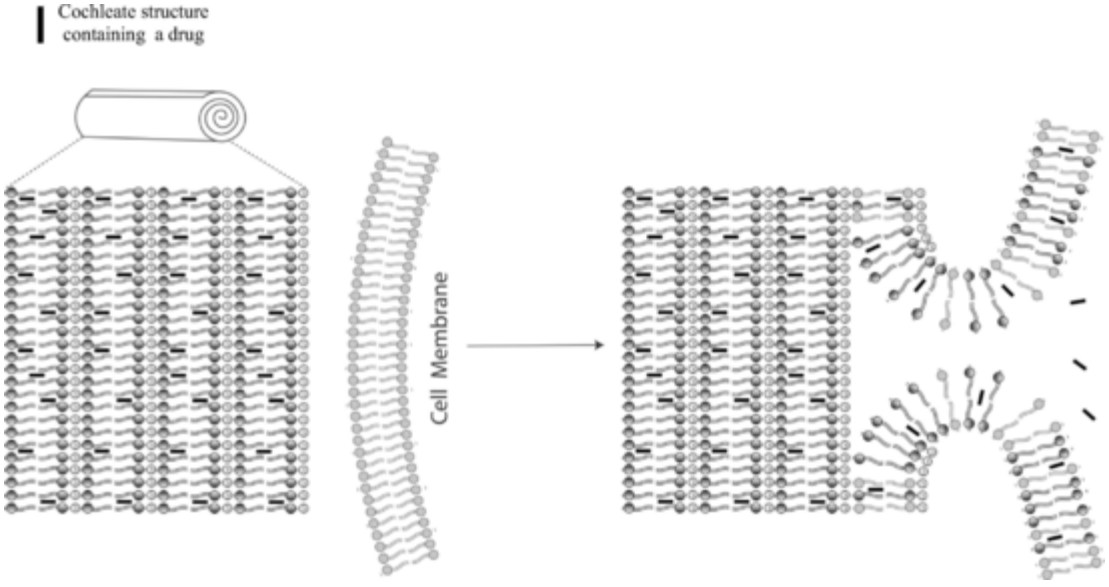

Fig. 7. Schematic representation of the interaction of cochleate particles with the cell membrane.

Appendix A. Supplementary material

Supplementary data to this article can be found online at https://doi.org/10.1016/j.ijpharm.2021.120688.

References

Aigner, M., Lass-Flörl, C., 2020. Encochleated Amphotericin B: is the oral availability of amphotericin B finally reached?. Journal of Fungi 6 (2), 66. https://doi.org/10.3390/jof6020066.

Andrieux, K., Forte, L., Lesieur, S., Paternostre, M., Ollivon, M., Grabielle-Madelmont, C., 2009. Solubilisation of dipalmitoylphosphatidylcholine bilayers by sodium taurocholate: A model to study the stability of liposomes in the gastrointestinal tract and their mechanism of interaction with a model bile salt. Eur. J. Pharm. Biopharm. 71, 346–355. https://doi.org/10.1016/j.ejpb.2008.09.004.

Barwicz, J., Christian, S., Gruda, I., 1992. Effects of the aggregation state of amphotericin B on its toxicity to mice. Antimicrob. Agents Chemother. 36 (10), 2310–2315. https://doi.org/10.1128/AAC.36.10.2310.

Barwicz, J., Beauregard, M., Tancrède, P., 2002. Circular dichroism study of interactions of Fungizone or Am Bisome forms of amphotericin B with human low density lipoproteins. Biopolymers 67 (1), 49–55. https://doi.org/10.1002/bip.10042.

Barwicz, J., Gruszecki, W.I., Gruda, I., 1993. Spontaneous organization of amphotericin B in aqueous medium. J. Colloid Interface Sci. 158 (1), 71–76. https://doi.org/10.1006/jcis.1993.1230.

Berman, J., 2005. Recent developments in leishmaniasis: epidemiology, diagnosis, and treatment. Current Infect. Dis. Rep. 7 (1), 33–38. https://doi.org/10.1007/s11908-005-0021-1.

Bozó, T., Wacha, A., Mihály, J., Bóta, A., Kellermayer, M.S.Z., 2017. Dispersion and stabilization of cochleate nanoparticles. Eur. J. Pharm. Biopharm. 117, 270–275. https://doi.org/10.1016/j.ejpb.2017.04.030.

Chattopadhyay, A., Jafurulla, M.d., 2011. A novel mechanism for an old drug: Amphotericin B in the treatment of visceral leishmaniasis. Biochem. Biophys. Res. Commun. 416 (1–2), 7–12. https://doi.org/10.1016/j.bbrc.2011.11.023.

Chaudhari, M.B., Desai, P.P., Patel, P.A., Patravale, V.B., 2016. Solid lipid nanoparticles of amphotericin B (AmbiOnp): In vitro and in vivo assessment towards safe and effective oral treatment module. Drug Delivery Translational Res. 6 (4), 354–364. https://doi.org/10.1007/s13346-015-0267-6.

Chen, Y.-C., Su, C.-Y., Jhan, H.-J., Ho, H.-O., Sheu, M.-T., 2015. Physical characterization and in vivo pharmacokinetic study of self-assembling amphotericin B-loaded lecithin-based mixed polymeric micelles. Int. J. Nanomed. 10, 7265–7274. https://doi.org/10.2147/IJN.S95194.

Dangi, J.S., Vyas, S.P., Dixit, V.K., 1998. Effect of various lipid-bile salt mixed micelles on the intestinal absorption of Amphotericin B in rat, Drug Develop. Ind. Pharm. 24, 631–635. https://doi.org/10.3109/03639049809082364.

David, G., Pérez, J., 2009. Combined sampler robot and high-performance liquid chromatography: a fully automated system for biological small-angle X-ray scattering experiments at the synchrotron SOLEIL SWING beamline. J. Applied Crystallography 42, 892–900. https://doi.org/10.1107/S0021889809029288.

Espada, R., Valdespina, S., Alfonso, C., Rivas, G., Ballesteros, M.P., Torrado, J.J., 2008. Effect of aggregation state on the toxicity of different amphotericin B preparations. Int. J. Pharm. 361 (1), 64–69. https://doi.org/10.1016/j.ijpharm.2008.05.013.

Faustino, Pinheiro, 2020. Lipid systems for the delivery of Amphotericin B in antifungal therapy. Pharmaceutics, 12(1), 29. https://doi.org/10.3390/pharmaceutics12010029

Gaboriau, F., Chéron, M., Petit, C., Bolard, J., 1997. Heat-induced superaggregation of amphotericin B reduces its in vitro toxicity: A new way to improve its therapeutic index. Antimicrob. Agents Chemother. 41 (11), 2345–2351. https://doi.org/10.1128/AAC.41.11.2345.

Garidel, P., Richter, W., Rapp, G., Blume, A., 2001. Structural and morphological investigations of the formation of quasi-crystalline phases of 1,2-dimyristoyl-sn-glycero-3- phosphoglycerol (DMPG). PCCP 3 (8), 1504–1513. https://doi.org/10.1039/b009881g.

Hamill, R.J., 2013. Amphotericin B formulations: A comparative review of efficacy and toxicity. Drugs 73 (9), 919–934. https://doi.org/10.1007/s40265-013-0069-4.

Hauser, H., Finer, E.G., Darke, A., 1977. Crystalline anhydrous Ca-phosphatidylserine bilayers. Biochem. Biophys. Res. Commun. 76 (2), 267–274. https://doi.org/10.1016/0006-291X(77)90721-5.

Hossain, Z., Konishi, M., Hosokawa, M., Takahashi, K., 2006. Effect of polyunsaturated fatty acid-enriched phosphatidylcholine and phosphatidylserine on butyrate-induced growth inhibition, differentiation and apoptosis in Caco-2 cells. Cell Biochem. Funct. 24 (2), 159–165. https://doi.org/10.1002/cbf.1202.

Huang, W., Zhang, Z., Han, X., Tang, J., Wang, J., Dong, S., Wang, E., 2002. Ion channel behavior of Amphotericin B in sterol-free and cholesterol- or ergosterol-containing supported phosphatidylcholine bilayer model membranes investigated by electrochemistry and spectroscopy. Biophys. J. 83 (6), 3245–3255. https://doi.org/10.1016/S0006-3495(02)75326-5.

Hubatsch, I., Ragnarsson, E.G.E., Artursson, P., 2007. Determination of drug permeability and prediction of drug absorption in Caco-2 monolayers. Nat. Protoc. 2 (9), 2111–2119. https://doi.org/10.1038/nprot.2007.303.

Hui, S.W., Boni, L.T., Stewart, T.P., Isac, T., 1983. Identification of phosphatidylserine and phosphatidylcholine in calcium-induced phase separated domains. Biochemistry 22 (14), 3511–3516. https://doi.org/10.1021/bi00283a032.

Ibrahim, F., Sivak, O., Wasan, E.K., Bartlett, K., Wasan, K.M., 2013. Efficacy of an oral and tropically stable lipid-based formulation of Amphotericin B (iCo-010) in an experimental mouse model of systemic candidiasis. Lipids Health Dis. 12 (1), 158. https://doi.org/10.1186/1476-511X-12-158.

Jain, S., Yadav, P., Swami, R., Swarnakar, N.K., Kushwah, V., Katiyar, S.S., 2018. Lyotropic liquid crystalline nanoparticles of Amphotericin B: Implication of phytantriol and glyceryl monooleate on bioavailability enhancement. AAPS PharmSciTech 19 (4), 1699–1711. https://doi.org/10.1208/s12249-018-0986-3.

Jin, T., Mannino, R. & Zarif, L., 2000. Nanocochleate formulations, process of preparation and method of delivery of pharmaceutical agents. US Patent US6153217A https://patents.google.com/patent/US6153217A/en.

Kelly, S. M. K. and Price N.C., 2000. The use of circular dichroism in the investigation of protein structure and function. Current Protein & Peptide Science, 1. http://www.eurekaselect.com/81742/article

Khan, M., Nadhman, A., Shah, W., Khan, I., Yasinzai, M., 2019. Formulation and characterisation of a self-nanoemulsifying drug delivery system of amphotericin B for the treatment of leishmaniasis. IET Nanobiotechnol. 13 (5), 477–483. https://doi.org/10.1049/iet-nbt.2018.5281.

Kowapradit, J., Opanasopit, P., Ngawhirunpat, T., Apirakaramwong, A., Rojanarata, T., Ruktanonchai, U., Sajomsang, W., 2010. In vitro permeability enhancement in intestinal epithelial cells (Caco-2) monolayer of water soluble quaternary ammonium chitosan derivatives. AAPS PharmSciTech 11 (2), 497–508. https://doi.org/10.1208/s12249-010-9399-7.

Lu, R., Hollingsworth, C., Qiu, J., Wang, A., Hughes, E., Xin, X., Konrath, K.M., Elsegeiny, W., Park, Y.-D., Atakulu, L., Craft, J.C., Tramont, E.C., Mannino, R., Williamson, P.R., 2019. Efficacy of oral encochleated Amphotericin B in a mouse model of cryptococcal meningoencephalitis. MBio 10 (3). https://doi.org/10.1128/mBio.00724-19.

Mannino, R. & Perlin, D., 2015. Oral dosing of encochleated amphotericin B (CAmB): rapid drug targeting to infected tissues in mice with invasive candidiasis. Scientific Presentations & Publications Matinas Biopharma 2015. Available online: https://www.matinasbiopharma.com/media/scientific-presentations-publications (accessed on 21 April 2021).

Ménez, C., Buyse, M., Besnard, M., Farinotti, R., Loiseau, P.M., Barratt, G., 2006a. Interaction between miltefosine and amphotericin B: consequences for their activities towards intestinal epithelial cells and *Leishmania donovani* promastigotes *in vitro*. Antimicrob. Agents Chemother. 50 (11), 3793–3800. https://doi.org/10.1128/AAC.00837-06.

Ménez, C., Buyse, M., Chacun, H., Farinotti, R., Barratt, G., 2006b. Modulation of intestinal barrier properties by miltefosine. Biochem. Pharmacol. 71 (4), 486–496. https://doi.org/10.1016/j.bcp.2005.11.008.

Menotti, J., Alanio, A., Sturny-Leclere, A., Vitry, S., Sauvage, F., Barratt, G., Bretagne, S., 2017. A cell impedance-based real-time *in vitro* assay to assess the toxicity of amphotericin B formulations. Toxicol. Appl. Pharmacol. 334, 18–23. https://doi.org/10.1016/j.taap.2017.08.017.

Moulin, M., Solgadi, A., Veksler, V., Garnier, A., Ventura-Clapier, R., Chaminade, P., 2015. Sex-specific cardiac cardiolipin remodelling after doxorubicin treatment. Biol. Sex Differences 6 (1), 20. https://doi.org/10.1186/s13293-015-0039-5.

Nagarsekar, K., Ashtikar, M., Steiniger, F., Thamm, J., Schacher, F., Fahr, A., 2016. Understanding cochleate formation: Insights into structural development. Soft Matter 12 (16), 3797–3809. https://doi.org/10.1039/C5SM01469G.

Nagarsekar, K., Ashtikar, M., Steiniger, F., Thamm, J., Schacher, F.H., Fahr, A., 2017. Micro-spherical cochleate composites: Method development for monodispersed cochleate system. J. Liposome Res. 27 (1), 32–40. https://doi.org/10.3109/08982104.2016.1149865.

No, J.H., 2016. Visceral leishmaniasis: Revisiting current treatments and approaches for future discoveries. Acta Trop. 155, 113–123. https://doi.org/10.1016/j.actatropica.2015.12.016.

Rochelle do Vale Morais, A.R., Silva, A. L., Cojean, S., Balaraman, K., Bories, C., Pomel, S., Barratt, G., do Egito, E. S. T., & Loiseau, P. M., 2018a. In-vitro and in-vivo antileishmanial activity of inexpensive Amphotericin B formulations: Heated Amphotericin B and Amphotericin B-loaded microemulsion. Experimental Parasitology, 192, 85–92. https://doi.org/10.1016/j.exppara.2018.07.017

Pawar, A., Bothiraja, C., Shaikh, K., Mali, A., 2015. An insight into cochleates, a potential drug delivery system. RSC Adv. 5 (99), 81188–81202. https://doi.org/10.1039/C5RA08550K.

Pham, T.T.H., Barratt, G., Michel, J.P., Loiseau, P.M., Saint-Pierre-Chazalet, M., 2013. Interactions of antileishmanial drugs with monolayers of lipids used in the development of amphotericin B–miltefosine-loaded nanocochleates. Colloids Surf. B 106, 224–233. https://doi.org/10.1016/j.colsurfb.2013.01.041.

Pham, T.T.H., Gueutin, C., Cheron, M., Abreu, S., Chaminade, P., Loiseau, P.M., Barratt, G., 2014. Development of antileishmanial lipid nanocomplexes. Biochimie 107, 143–153. https://doi.org/10.1016/j.biochi.2014.06.007.

Santangelo, R., Paderu, P., Delmas, G., Chen, Z.-W., Mannino, R., Zarif, L., Perlin, D.S., 2000. Efficacy of oral cochleate-Amphotericin B in a mouse model of systemic candidiasis. Antimicrob. Agents Chemother. 44 (9), 2356–2360. https://doi.org/10.1128/AAC.44.9.2356-2360.2000.

Serrano, D.R., Lalatsa, A., Dea-Ayuela, M.A., Bilbao-Ramos, P.E., Garrett, N.L., Moger, J., Guarro, J., Capilla, J., Ballesteros, M.P., Schätzlein, A.G., Bolás, F., Torrado, J.J., Uchegbu, I.F., 2015. Oral particle uptake and organ targeting drives the activity of Amphotericin B nanoparticles. Mol. Pharm. 12 (2), 420–431. https://doi.org/10.1021/mp500527x.

Shervani, Z., Etori, H., Taga, K., Yoshida, T., Okabayashi, H., 1996. Aggregation of polyene antibiotics as studied by electronic absorption and circular dichroism spectroscopies. Colloids Surf. B 7 (1), 31–38. https://doi.org/10.1016/0927-7765(96)01283-0.

Thanki, K., Date, T., Jain, S., 2019. Improved oral bioavailability and gastrointestinal stability of Amphotericin B through fatty acid conjugation approach. Mol. Pharm. 16 (11), 4519–4529. https://doi.org/10.1021/acs.molpharmaceut.9b00662.

Torres-Guerrero, E., Quintanilla-Cedillo, M. R., Ruiz-Esmenjaud, J., & Arenas, R., 2017. Leishmaniasis: A review. F1000Research, 6, 750. https://doi.org/10.12688/f1000research.11120.

Wasan, K.M., Kennedy, A.L., Cassidy, S.M., Ramaswamy, M., Holtorf, L., Chou, J.W., Pritchard, P.H., 1998. Pharmacokinetics, distribution in serum lipoproteins and tissues, and renal toxicities of amphotericin B and Amphotericin B Lipid Complex in a hypercholesterolemic rabbit model: single-dose studies. Antimicrob. Agents Chemother. 42 (12), 3146–3152. https://doi.org/10.1128/AAC.42.12.3146.

Yang, Z., Chen, M., Yang, M., Chen, J., Fang, W., Xu, P., 2014. Evaluating the potential of cubosomal nanoparticles for oral delivery of amphotericin B in treating fungal infection. Int. J. Nanomed. 9, 327–336. https://doi.org/10.2147/IJN.S54967.

Zarif, L., Graybill, J.R., Perlin, D., Najvar, L., Bocanegra, R., Mannino, R.J., 2000. Antifungal activity of Amphotericin B cochleates against Candida albicans infection in a mouse model. Antimicrob. Agents Chemother. 44 (6), 1463–1469. https://doi.org/10.1128/AAC.44.6.1463-1469.2000.